TRAVELLING WAVES IN TWO-DIMENSIONAL PLANE POISEUILLE FLOW

WARREN R. SMITH* AND JAN G. WISSINK†

Abstract. The asymptotic structure of laminar modulated travelling waves in two-dimensional high-Reynolds-number plane Poiseuille flow is investigated on the upper-energy branch. A finite set of independent slowly varying parameters are identified which parameterize the solution of the Navier–Stokes equations in this subset of the phase space. Our parameterization of the weakly stable modes describes an attracting manifold of maximum-entropy configurations. The complementary modes, which have been neglected in this parameterization, are strongly damped. In order to seek a closure, a countably infinite number of modulation equations are derived on the long viscous time scale: a single equation for averaged kinetic energy and momentum; and the remaining equations for averaged powers of vorticity. Only a finite number of these vorticity modulation equations are required to determine the finite number of unknowns. The new results show that the evolution of the slowly varying amplitude parameters is determined by the vorticity field and that the phase velocity responds to these changes in the amplitude in accordance with the kinetic energy and momentum. The new results also show that the most crucial physical mechanism in the production of vorticity is the interaction between vorticity and kinetic energy, this interaction being responsible for the existence of the attractor.

Key words. strongly nonlinear analysis, travelling waves, Navier–Stokes equations

AMS subject classifications. 35B25, 76D33

1. Introduction. A central challenge for Navier–Stokes analysis is to derive the equations for the long length scales and long time scales directly from the equations of motion. This point was recognized as the fifth open problem in Kolmogorov's 1958 seminar on dynamical systems and hydrodynamic stability which refers to "the mathematical theory of partial differential equations containing a small parameter multiplying the term with the highest derivative; until now only such phenomena as boundary layers or interior layers have been studied." [1] This article develops a formal perturbation scheme to investigate the existence of a self-consistent laminar closure; the asymptotic approach adopted being to describe the long time scales of the Navier–Stokes equations on a strongly nonlinear upper-energy branch. After many decades of intensive research on the application of asymptotic analysis to fluid mechanics, this is an ambitious objective. Accordingly, the simplest physical situation is adopted; that is, a finite-amplitude modulated nonlinear travelling wave. Furthermore, fluid mechanics is better understood in two dimensions than in three, this being a compelling reason for adopting it as a starting point. The important case of two-dimensional plane Poiseuille flow, which is modulated on the long viscous time-scale, will provide a particular example of the closure problem.

A second motivation is to develop simple analytical formulae for high-Reynolds-number flows, our aspiration being to find a generalization of the Landau equation for the modulated strongly nonlinear travelling waves on the upper-energy branch in two-dimensional plane Poiseuille flow. This open problem of a generalization of the Landau equation was originally posed in the literature more than two decades ago [13]. Although such a model will inevitably be restricted in its scope, simple formulae provide valuable physical insight into the large scales which would be limited from more general alternative approaches such as direct numerical simulation or proper orthogonal decomposition.

A third motivation for the study of two-dimensional plane Poiseuille flow is that it is an important intermediate stage in the instability process of three-dimensional plane Poiseuille flow [23]. In this instability process, the formation of the secondary flow corresponds to two-dimensional quasi-steady travelling waves, which have recently been shown to be maximum-entropy configurations [33]. We seek to gain further insight into the dynamics of these quasi-steady states.

Two-dimensional plane Poiseuille flow with constant streamwise pressure gradient and periodic boundary conditions is considered. The basic flow becomes linearly unstable at a Reynolds number of 5772 (see Figure 1(a)). Below the critical Reynolds number, formal perturbation theory has shown that the flow is nonlinearly unstable: the domain of attraction shrinks as the Reynolds number increases [4]. Finite-amplitude travelling waves have been demonstrated numerically for a Reynolds number greater than approximately 2900 and a finite band of wavenumbers [11], there being either zero or two finite-amplitude travelling waves at subcritical Reynolds numbers on this neutral surface. In the case when there are two, the lower-energy branch is unstable while the upper-energy branch is stable (see Figure 1(b)). For the case of supercritical Reynolds number, the lower-energy branch bifurcates from the basic flow (see Figure 1(c)). The trajectory of each initial condition within the basin of attraction of the stable branch exhibits two behaviours: firstly, an evolution on the short convective time scale to a manifold of quasi-steady travelling waves; and secondly, an approach to the travelling wave on the slow viscous time scale [22].

*School of Mathematics, The University of Birmingham, Edgbaston, Birmingham, B15 2TT, UK. (W.Smith@bham.ac.uk).
†School of Engineering and Design, Brunel University, Uxbridge, Middlesex, UB8 3PH, UK. (Jan.Wissink@brunel.ac.uk).

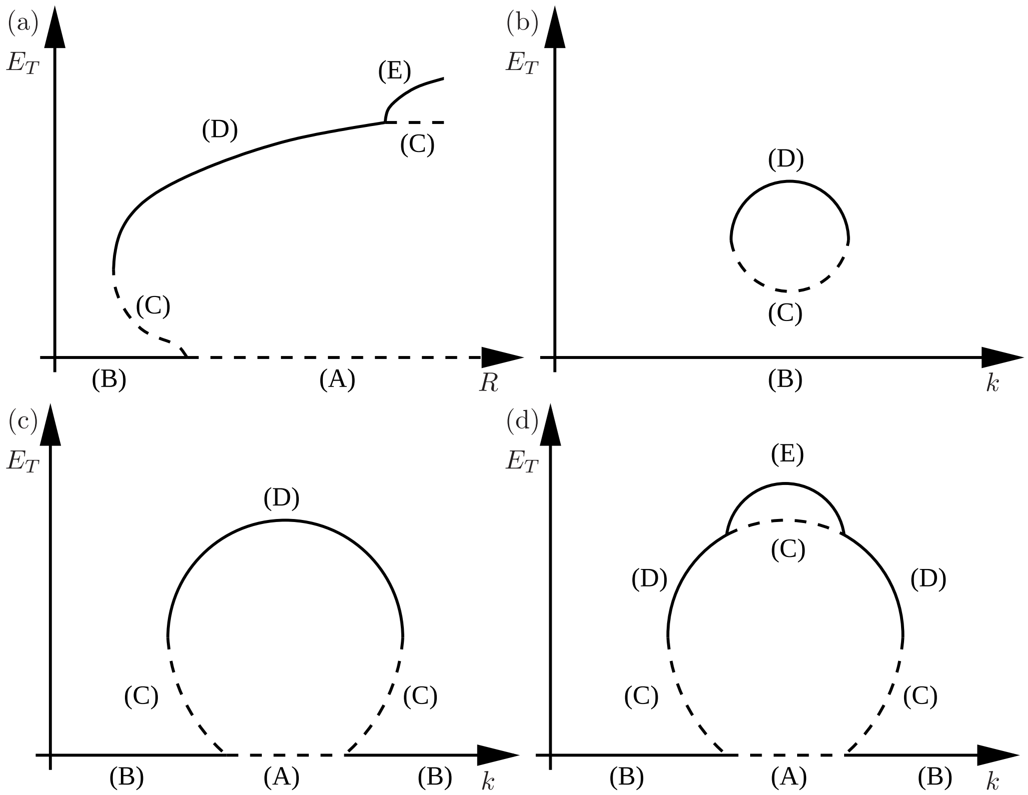

FIG. 1. *Four schematic slices of the bifurcation diagram for two-dimensional plane Poiseuille flow in* (E_T, R, k) *space (a) at a constant streamwise wavenumber, (b) at Reynolds number* $2900 < R < 5772$*, (c) at Reynolds number* $R > 5772$ *and below the first Hopf bifurcation and (d) at Reynolds number above the first Hopf bifurcation and below the second: (A) unstable basic flow, (B) stable basic flow, (C) unstable single-phased wave, (D) stable single-phased wave and (E) stable two-phased wave. The total dimensionless kinetic energy relative to the basic flow is* E_T*, the Reynolds number is* R *and dimensionless streamwise wavenumber is* k*.*

The weakly nonlinear analysis of waves in plane Poiseuille flow relied for many years on expansions in the amplitude, this research being initiated by the seminal work in [34]. It has successfully predicted the evolution of small-amplitude modulated travelling waves governed by the Landau equation near the critical Reynolds number of 5772.

An elegant method for the analysis of slowly-varying non-dissipative wave trains is known as Whitham's method [36], this being based on an averaged Lagrangian formulation. Whitham's method may be considered as more general than a weakly nonlinear analysis: the latter is restricted to weak modulations about a fixed frequency and wavenumber. Conversely, weakly nonlinear analysis may be considered to be more general than Whitham's method: the latter does not apply to dissipative flows where the Lagrangian is absent. Extensions of Whitham's method have been proposed for dissipative systems: (i) The problem of resonant interaction of a triad of wave modes in a parallel shear flow was considered in [35]. A variational formulation of the incompressible Navier–Stokes equations was utilised, but it involved additional dependent variables which have no direct physical significance. (ii) The pseudo-variational principle of Prigogine was used in [14]. In this case, the Lagrangian depended on the function to be varied and the solution. This technique was not applied to the Navier–Stokes equations. (iii) The evolution of a high-frequency wave packet in an unsteady flow was modelled in [12], a similar extension being reported by [18]. In summary, these extensions of Whitham's method have had limited success in deriving the modulation equations for finite-amplitude waves described by the Navier–Stokes equations. Accordingly, we propose an alternative approach; that is, removal of the restrictions placed on the multiple scale analysis.

Kuzmak [17] introduced the idea of an asymptotic analysis based on two time scales for strongly nonlinear oscillators: at leading order, the amplitude dependence of the frequency was determined; and at next order, an ordinary differential equation for the amplitude was obtained. Luke [19] extended Kuzmak's ideas to strongly nonlinear dispersive waves with oscillatory solutions, an amplitude dependent dispersion relation and a partial differential equation for the amplitude being deduced. The developments of Luke need to be viewed in the context of Whitham's averaged Lagrangian method in which the same results were obtained in a simpler manner. The appendix written by King in [31] demonstrated how implicit modulation equations, which are produced by the method of Kuzmak-Luke, could be rewritten in an explicit form.

TABLE 1
Summary of the strengths and weaknesses of analytical methods in determining the modulation equations for travelling waves in fluid flow.

	Large-amplitude wave	Dissipative flow
Whitham's method	Straightforward to apply when a Lagrangian is available	Limited extensions
Weakly nonlinear analysis	No	Yes
Strongly nonlinear analysis	Practical difficulty in solving an adjoint problem and determining modulation equations	Yes
Boundary-layer analysis	Restricted to wall-bounded flows	Yes

The method of Kuzmak-Luke was first applied to the Navier–Stokes equations using the Fredholm alternative [29], modulation equations being derived for each linearly independent vector in the null space of the adjoint problem. Unfortunately, this approach did not determine equations for the amplitude of the oscillations of a viscous drop: the vectors in the null space of the adjoint problem had to be utilized in conjunction with the transport theorem to eliminate correction terms [30]. In this article, the latter approach will again be required to evaluate modulation equations for travelling waves in two-dimensional plane Poiseuille flow. We note that an oversimplified parity assumption was made in the analysis of plane Poiseuille flow in [29]; this matter is properly dealt with here.

Strongly nonlinear analysis or the method of Kuzmak-Luke may be considered to be more general than Whitham's method and weakly nonlinear analysis: the former applies to dissipative flows and it is not restricted to weak modulations. On the other hand, there are mathematical obstacles which have limited the application of strongly nonlinear analysis to the Navier–Stokes equations: a matrix adjoint problem must be solved analytically and the Fredholm alternative may not always be applied. Despite the mathematical difficulty, the physical insight into the Navier–Stokes equations makes the rewards substantial. The challenges of hydrodynamic instability require a technique for large-amplitude waves with dissipation. Only strongly nonlinear analysis can meet these requirements (see the summary in Table 1).

A solution of the leading-order outer problem is required. In this article, the leading-order outer problem is the two-dimensional Euler equations in a reference frame moving with the phase velocity. A general solution to this problem has never been found; nevertheless, the task of identifying independent slowly varying parameters will be undertaken. We are assisted in this regard by the recent discovery of a first integral to this problem [33], the vorticity-stream function relationship corresponding to a Joyce–Montgomery equation [16, 20, 21] which had been anticipated by [15]. Three slowly varying parameters are found in this first integral: the phase velocity and two amplitude parameters. In the subsequent analysis of the leading-order problem, we must ensure that all of the symmetry groups are exploited; otherwise, redundant slowly varying parameters would be derived and the modulation equations could be incorrectly labelled as an underdetermined system.

A counterpart to plane Poiseuille flow is the uniform flow over a semi-infinite plate in two dimensions which has been extensively studied over many years. In [27], the progress of an initially small unstable Tollmien-Schlichting disturbance at high frequency has been charted in the boundary layer. The results were summarized on a schematic amplitude diagram in Figure 3 of [27], this amplitude-dependent neutral curve being closed in Figure 4 of [28]. These two figures have some striking similarities with Figure 1(c).

(i) The subcritical bifurcation from the basic flow in Figure 1(c) compares with a supercritical bifurcation in Figure 3 of [27]. On this branch, Smith and Burggraf [27] described stable Tollmien-Schlichting modes by triple-deck theory, then a restricted range of mode amplitudes by the Benjamin-Ono equation and, finally, the largest wave amplitudes by the unsteady Euler equations. The latter two amplitude ranges were found to be subject to bursts of vorticity from the sublayer adjacent to the boundary [8].

(ii) The supercritical bifurcation in Figure 1(c) compares with a second supercritical bifurcation in Figure 3 of [27], which is described by nonlinear critical layers [3, 26]. These solution branches are unstable in both cases [9].

There are also some notable differences.

(i) In Figure 3 of [27] and Figure 4 of [28], the flow does not resemble the travelling waves on the upper-energy branch in Figure 1(c) which are under investigation.

(ii) In Figure 1(c), the wavenumber is bounded between 1/2 and 2; whereas, boundary-layer theory predicts a much larger range of wavenumbers in Figure 4 of [28].

This boundary-layer analysis was extended to other wall-bounded flows; most notably, Smith and Bodonyi [25] derived a remarkable nonlinear helical travelling wave solution in Hagen-Poiseuille flow. Their high-Reynolds-number strongly nonlinear asymptotic study stands out because the amplitude of the neutral mode was explicitly determined, this solution having been recently confirmed as a numerically exact solution of the Navier–Stokes equations [5]. The kinetic energy of this solution relative to the basic flow is asymptotically small for large Reynolds number; however, our interest is in the case of order one kinetic energy which corresponds to the upper-energy branch in this article.

The contents of the paper will now be outlined. In section 2, formal perturbation theory is applied to the quasi-steady travelling waves in two-dimensional plane Poiseuille flow. The leading-order problem is integrated once to obtain a sinh-Poisson equation for the stream function. The boundary, parity and symmetry conditions are then utilized to convert this partial differential equation into a finite set of ordinary differential equations. At next order, modulation equations are derived using linearly independent vectors in the null space of the adjoint and the transport theorem. The modulation equations for momentum and kinetic energy must be combined in order to eliminate a correction term. The Weierstrass approximation theorem is required to form a countably infinite number of vorticity modulation equations from the uncountably infinite number of vectors in the null space of the adjoint. Section 3 interprets the modulation equations in terms of the fluid mechanics. Extensions to the three-dimensional problem and two-phased waves are also considered. Section 4 studies the high-temperature limit, which highlights the role of nonlinearities in the vorticity-stream function relationship. Finally, section 5 gives a brief discussion of the results.

2. Asymptotic analysis.

2.1. Mathematical model. We define $2h$ to be the channel width, μ the dynamic viscosity, ρ the density, $-G$ the constant pressure gradient and $U^* = Gh^2/2\mu$. We transform to dimensionless variables via

$$x^* = hx, \qquad y^* = hy, \qquad t^* = \frac{ht}{U^*}, \qquad u^* = U^*u, \qquad v^* = U^*v, \qquad p^* = \rho {U^*}^2 p,$$

where $(x^*, y^*)^T$ are the spatial coordinates, t^* is time, $\boldsymbol{q}^* = (u^*, v^*)^T$ are the fluid velocities and p^* is pressure. The two-dimensional Navier–Stokes and continuity equations become

$$\frac{\partial \boldsymbol{q}}{\partial t} + (\boldsymbol{q}\cdot\boldsymbol{\nabla})\boldsymbol{q} + \boldsymbol{\nabla} p = \epsilon\left[\nabla^2\boldsymbol{q} + 2\hat{\boldsymbol{x}}\right] \tag{2.1}$$

and

$$\boldsymbol{\nabla}\cdot\boldsymbol{q} = 0, \tag{2.2}$$

in which $0 < \epsilon \ll 1$ is the reciprocal of the Reynolds number $R = h^3G/2\rho\nu^2$, $\nu = \mu/\rho$, $\boldsymbol{q}$ is the velocity vector $(u, v)^T$ and $\hat{\boldsymbol{x}}$ is the unit vector along the x-axis. The boundary conditions are

$$\boldsymbol{q}(x, \pm 1, t) = 0, \qquad \boldsymbol{q}(0, y, t) = \boldsymbol{q}(2\pi/k, y, t), \tag{2.3}$$

where k is the constant streamwise wavenumber. The case of a long periodic box ($k \ll 1$) is discussed in Section 3.2. We assume that the initial conditions with $\epsilon = 0$ are consistent with a travelling wave solution. Moreover, the desired single-phased wave possesses a shift-and-reflect symmetry of the form

$$(u, v)(x, y, t) = (u, -v)(x + \pi/k, -y, t).$$

The validity of this symmetry assumption is demonstrated in Figure 2 in which a snapshot of a quasi-steady travelling wave is plotted with $\epsilon = 1.1 \times 10^{-4}$ and $k = 1.1$. The numerical method described in [33] has been employed on a 300×300 mesh.

Equations (2.1)-(2.2) can be written in the form

$$\frac{\partial u}{\partial t} + \frac{\partial}{\partial x}(u^2) + \frac{\partial}{\partial y}(uv) + \frac{\partial p}{\partial x} = \epsilon\left[\frac{\partial^2 u}{\partial x^2} + \frac{\partial^2 u}{\partial y^2} + 2\right], \tag{2.4}$$

or in the form,

$$\frac{\partial E}{\partial t} + \frac{\partial}{\partial x}(u[p+E]) + \frac{\partial}{\partial y}(v[p+E]) = \epsilon\frac{\partial}{\partial x}(v\omega) - \epsilon\frac{\partial}{\partial y}(u\omega) - \epsilon\omega^2 + 2\epsilon u, \tag{2.5}$$

or in the form,

$$\frac{\partial}{\partial t}(\omega^m) + \frac{\partial}{\partial x}(u\omega^m) + \frac{\partial}{\partial y}(v\omega^m) = \epsilon m\omega^{m-1}\left[\frac{\partial^2\omega}{\partial x^2} + \frac{\partial^2\omega}{\partial y^2}\right], \tag{2.6}$$

where kinetic energy is defined by $E = \boldsymbol{q}\cdot\boldsymbol{q}/2$, vorticity is defined by $\omega = \partial v/\partial x - \partial u/\partial y$ and $m > 1$. The analysis which follows will show that the reformulations (2.4)-(2.6) are the appropriate ones to consider.

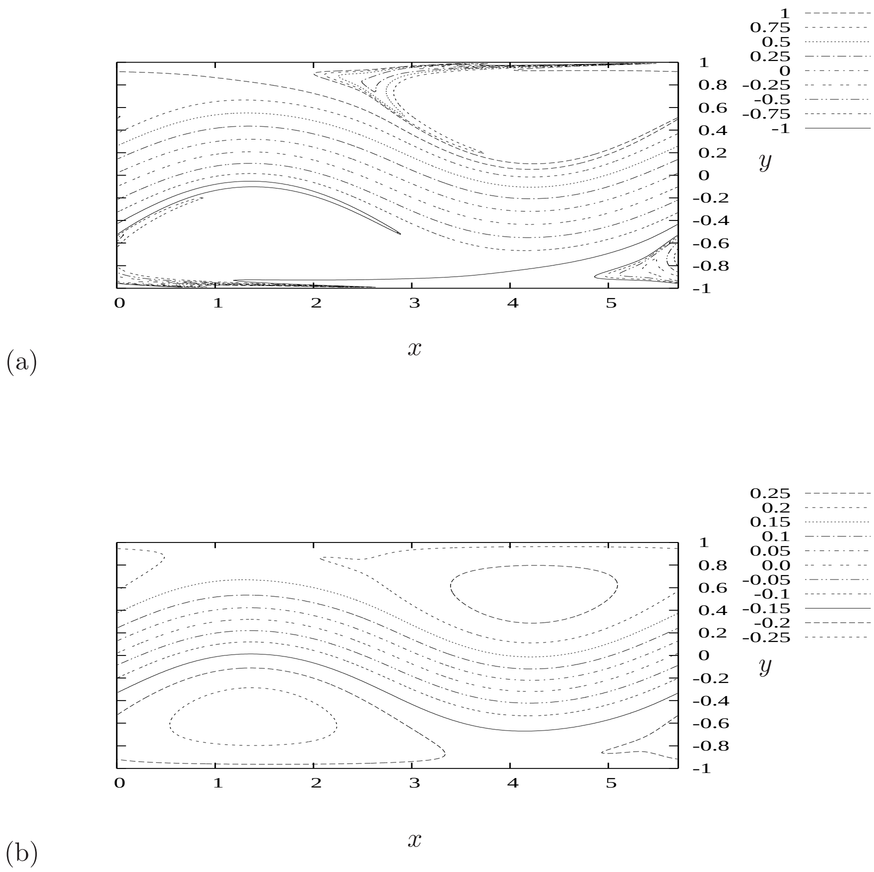

FIG. 2. *Snapshot of vorticity contours (a) and streamlines (b) for a quasi-steady single-phased travelling wave with* $\epsilon = 1.1 \times 10^{-4}$ *(*$R = 9000$*) and* $k = 1.1$ *plotted in a coordinate system moving with the phase velocity.*

2.2. The leading-order outer problem. We consider the outer region in which the leading-order problem is inviscid. The boundary layer and any other singular region is located outside of the region. We adopt a fast phase θ defined by $\theta_x = k$ and $\theta_t = -\sigma(\tilde{t})$ and a slow time scale $\tilde{t} = \epsilon t$, where σ is a local frequency. We introduce expansions of the form

$$u \sim u_0(\theta, y, \tilde{t}) + \epsilon u_1(\theta, y, \tilde{t}), \qquad v \sim v_0(\theta, y, \tilde{t}) + \epsilon v_1(\theta, y, \tilde{t}), \qquad p \sim p_0(\theta, y, \tilde{t}) + \epsilon p_1(\theta, y, \tilde{t}),$$

$$E \sim E_0(\theta, y, \tilde{t}) + \epsilon E_1(\theta, y, \tilde{t}), \qquad \omega \sim \omega_0(\theta, y, \tilde{t}) + \epsilon \omega_1(\theta, y, \tilde{t}),$$

as $\epsilon \to 0$. At leading order, we have

$$\bar{L}u_0 + k\frac{\partial p_0}{\partial \theta} = 0, \tag{2.7a}$$

$$\bar{L}v_0 + \frac{\partial p_0}{\partial y} = 0, \tag{2.7b}$$

$$k\frac{\partial u_0}{\partial \theta} + \frac{\partial v_0}{\partial y} = 0, \tag{2.7c}$$

with the differential operator

$$\bar{L} = (ku_0 - \sigma)\frac{\partial}{\partial \theta} + v_0\frac{\partial}{\partial y},$$

the periodic boundary conditions

$$[u_0, v_0, p_0](\theta + \Psi = 0, y, \tilde{t}) = [u_0, v_0, p_0](\theta + \Psi = 2\pi, y, \tilde{t}), \tag{2.8}$$

and the phase shift $\Psi(\tilde{t})$. The centre of an eddy adjacent to $y = 1$ is defined to be $\theta + \Psi = 0$ and the centre of the next eddy adjacent to $y = 1$ corresponds to $\theta + \Psi = 2\pi$, as shown in Figure 2(b). The centre of the intermediate counter-rotating eddy adjacent to $y = -1$ coincides with $\theta + \Psi = \pi$. We note that (2.7) are phase reversible; that is, invariant under $\theta + \Psi \to -(\theta + \Psi)$ and $v_0 \to -v_0$. Solutions are anticipated such that u_0 and p_0 (v_0) are even (odd) about the zeros of v_0. We have parity conditions

$$[u_0, p_0](\theta + \Psi, y, \tilde{t}) = [u_0, p_0](2\pi - (\theta + \Psi), y, \tilde{t}), \qquad v_0(\theta + \Psi, y, \tilde{t}) = -v_0(2\pi - (\theta + \Psi), y, \tilde{t}).$$

The shift-and-reflect symmetry becomes

$$(u_0, v_0)(\theta + \Psi, y, \tilde{t}) = (u_0, -v_0)(\theta + \Psi + \pi, -y, \tilde{t}).$$

We take the curl of (2.7a)-(2.7b) to obtain $\bar{L}\omega_0 = 0$. A stream function $\bar{\psi}$ is defined by the equations

$$u_0 = \frac{\partial \bar{\psi}}{\partial y}, \qquad v_0 = -k\frac{\partial \bar{\psi}}{\partial \theta},$$

so that (2.7c) is satisfied and the vorticity equation may be rewritten as

$$\frac{\partial}{\partial y}(\bar{\psi} - Uy)\frac{\partial \omega_0}{\partial \theta} - \frac{\partial}{\partial \theta}(\bar{\psi} - Uy)\frac{\partial \omega_0}{\partial y} = 0, \tag{2.9}$$

where $U = \sigma/k$. The first integral of (2.9) is the nonlinear Poisson equation

$$\omega_0 = -\Delta_0 \bar{\psi} = V(\bar{\psi} - Uy; A(\tilde{t}), B(\tilde{t}), \ldots), \tag{2.10}$$

in which the functional V must be determined, $A(\tilde{t}), B(\tilde{t}), \ldots$ are slowly varying parameters and

$$\Delta_0 = k^2\frac{\partial^2}{\partial \theta^2} + \frac{\partial^2}{\partial y^2}.$$

It has been show that the appropriate functional is the two-sign Joyce–Montgomery equation (see [16, 20, 21, 33]). We adopt this equation in the form

$$V(\phi; A(\tilde{t}), B(\tilde{t})) = A(\tilde{t}) \sinh\left(B(\tilde{t})\,\phi\right).$$

For example, a least-squares fit determines the slowly varying parameters $A = 0.673$, $B = 6.43$ and $U = 0.3107$ for the quasi-steady travelling wave shown in Figure 2. The Joyce–Montgomery equation occurs in a manifold of maximum-entropy configurations. This manifold is a trapping region in phase space: any trajectory leaving it would have decreased entropy which is a contradiction. Therefore, the manifold of maximum-entropy configurations is an attracting subset of the stable manifold in phase space (see Figure 3).

After the transformation $\psi = \bar{\psi} - Uy$, equation (2.10) becomes

$$-\Delta_0 \psi = A \sinh(B\,\psi) \tag{2.11}$$

with the periodic boundary condition

$$\psi\left(\theta + \Psi(\tilde{t}), y; A(\tilde{t}), B(\tilde{t}), \ldots\right) = \psi\left(\theta + \Psi(\tilde{t}) - 2n\pi, y; A(\tilde{t}), B(\tilde{t}), \ldots\right), \tag{2.12}$$

the parity

$$\psi\left(\theta + \Psi(\tilde{t}), y; A(\tilde{t}), B(\tilde{t}), \ldots\right) = \psi\left(2\pi - (\theta + \Psi(\tilde{t})), y; A(\tilde{t}), B(\tilde{t}), \ldots\right), \tag{2.13}$$

the shift-and-reflect symmetry condition

$$\psi\left(\theta + \Psi(\tilde{t}), y; A(\tilde{t}), B(\tilde{t}), \ldots\right) = -\psi\left(\theta + \Psi(\tilde{t}) + \pi, -y; A(\tilde{t}), B(\tilde{t}), \ldots\right) \tag{2.14}$$

and integer n. We also note that ψ is even about $\theta + \Psi = n\pi$. Using (2.11), equations (2.7a) and (2.7b) may be integrated once to obtain the leading-order pressure

$$p_0 = C - \frac{A}{B}\cosh(B\,\psi) - \frac{k^2}{2}\left(\frac{\partial \psi}{\partial \theta}\right)^2 - \frac{1}{2}\left(\frac{\partial \psi}{\partial y}\right)^2, \tag{2.15}$$

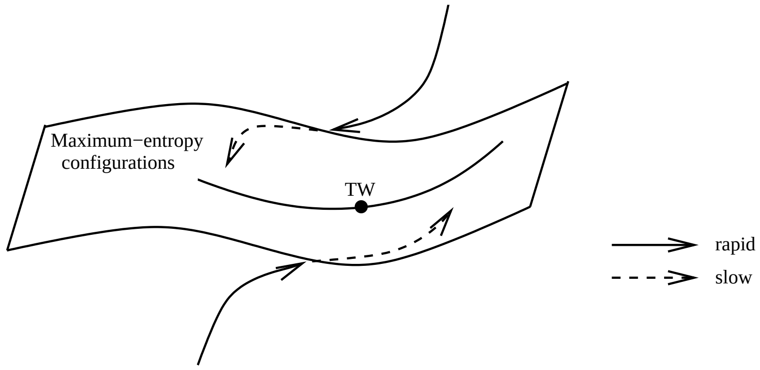

FIG. 3. *A schematic of the finite-dimensional attracting set of maximum-entropy configurations in phase space (denoted by a curved surface). The two-dimensional surface of single-phased travelling waves on the upper-energy branch lies within this attracting set (denoted by a solid line). All neighbouring trajectories rapidly enter this trapping region before slowly approaching the point in phase space corresponding to the travelling wave TW which is stable at a particular value of k and R (denoted by a large dot).*

where $C(\tilde{t})$ is an additional slowly varying parameter. Furthermore, this parameter may be set to zero without loss of generality. The interchange between the kinetic and internal energy on the short time scale is represented in (2.15).

The periodicity and parity conditions allow us to express the stream function as a Fourier cosine series

$$\psi = \sum_{l=0}^{\infty} c_l(y; A(\tilde{t}), B(\tilde{t}), \ldots) \cos(l(\theta + \Psi)). \tag{2.16}$$

If we substitute (2.16) into the sinh-Poisson equation (2.11), then we obtain

$$\sum_{l=0}^{\infty} \left[\frac{\partial^2 c_l}{\partial y^2} - k^2 l^2 c_l \right] \cos(l(\theta + \Psi)) + A \sinh(B \sum_{l=0}^{\infty} c_l \cos(l(\theta + \Psi))) = 0.$$

Coefficients in the Fourier cosine series are determined by utilising orthogonality. We deduce an infinite system of ordinary differential equations

$$\frac{\partial^2 c_0}{\partial y^2} + \frac{1}{2\pi} \int_{\theta=-\Psi}^{2\pi-\Psi} A \sinh\left(B \sum_{l=0}^{\infty} c_l \cos(l(\theta + \Psi)) \right) \mathrm{d}\theta = 0$$

and

$$\frac{\partial^2 c_j}{\partial y^2} - k^2 j^2 c_j + \frac{1}{\pi} \int_{\theta=-\Psi}^{2\pi-\Psi} A \sinh\left(B \sum_{l=0}^{\infty} c_l \cos(l(\theta + \Psi)) \right) \cos(j(\theta + \Psi)) \mathrm{d}\theta = 0,$$

where j is a natural number. However, only a finite number of the c_l are non-zero because viscous effects would reappear at leading order when $l = \mathcal{N} = \mathcal{O}(R^{1/2})$. For definiteness, we assume $c_l = 0$ for $l > \mathcal{N}$. The manifold of maximum-entropy configurations in Figure 3 is contained within a finite-dimensional volume in phase space.

The shift-and-reflect symmetry condition (2.14) requires that c_l is odd in y when l is even and c_l is even in y when l is odd. The second-order ordinary differential equations for c_l only have one degree of freedom each. We define this degree of freedom to be

$$\frac{\partial c_l}{\partial y}(y = 0) = \alpha_l(\tilde{t}) \tag{2.17}$$

for l even and

$$c_l(y = 0) = \alpha_l(\tilde{t}) \tag{2.18}$$

for l odd, where $\{\alpha_l(\tilde{t}) : l \in \mathbb{Z} \text{ and } 0 \le l \le \mathcal{N}\}$ are a finite set of slowly varying unknowns. The numerical solution described in [33] may be exploited to validate the symmetry conditions applied to the leading-order outer problem. The travelling wave is investigated using the simulation on a 200×200 mesh with $\epsilon = 2.5 \times 10^{-4}$ and $k = 1.25$. The coefficients in the Fourier cosine series are evaluated using standard techniques. In Figure 4, the values of c_0, c_1, c_2 and c_3 are shown for this periodic steady state. We note that the parity in y is correctly predicted by our analysis. The correction terms in the asymptotic analysis may not be perceived in the figure as ϵ is so small.

It remains to determine a set of modulation equations for the slowly varying parameters A, B, U, α_0, α_1, …, $\alpha_{\mathcal{N}-1}$ and $\alpha_{\mathcal{N}}$.

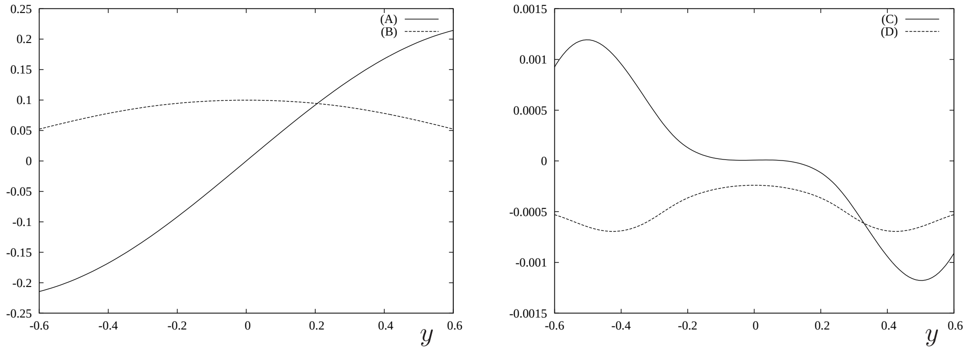

FIG. 4. *Coefficients in the Fourier cosine series for the travelling wave with* $\epsilon = 2.5 \times 10^{-4}$ *(*$R = 4000$*) and* $k = 1.25$*: (A)* c_0 *is an odd function of* y*, (B)* c_1 *an even function of* y*, (C)* c_2 *an odd function of* y *and (D)* c_3 *an even function of* y*.*

2.3. The boundary-layer problem. The solution of the leading-order outer problem will be inconsistent with the boundary conditions (2.3). Boundary layers are required to describe the significance of viscous effects near the walls. The boundary layers may exert a controlling influence on the flow as a whole or they may provide a smooth transition between the inviscid body of the flow and the no-slip boundary condition. We are concerned with the description of the latter category. In the interest of brevity, we will not discuss it any further, but return to the derivation of the modulation equations for the slow evolution represented by the dashed line in Figure 3.

2.4. Modulation equations. In this section, the linear differential operators for the first correction and adjoint are stated (see [29]). Five linearly independent solutions to the adjoint problem are then deduced, only three of these resulting in physically meaningful modulation equations. A version of the momentum and kinetic energy modulation equations were first derived in [29]. However, a parity assumption was made on the exact solution; that is, u and p even about the half period and v odd about the half period. Subsequent accurate numerical simulations [33] have been used to show that this assumption only holds at leading order. These two modulation equations will need to be derived again.

At next order, we obtain

$$L\boldsymbol{z} = \begin{pmatrix} -\dfrac{\partial u_0}{\partial \tilde{t}} + \Delta_0 u_0 + 2 \\ -\dfrac{\partial v_0}{\partial \tilde{t}} + \Delta_0 v_0 \\ 0 \end{pmatrix}, \tag{2.19}$$

in which

$$L = \begin{pmatrix} \bar{L} + k\dfrac{\partial u_0}{\partial \theta} & \dfrac{\partial u_0}{\partial y} & k\dfrac{\partial}{\partial \theta} \\ k\dfrac{\partial v_0}{\partial \theta} & \bar{L} + \dfrac{\partial v_0}{\partial y} & \dfrac{\partial}{\partial y} \\ k\dfrac{\partial}{\partial \theta} & \dfrac{\partial}{\partial y} & 0 \end{pmatrix}, \qquad \boldsymbol{z} = \begin{pmatrix} u_1 \\ v_1 \\ p_1 \end{pmatrix},$$

with the periodic boundary conditions

$$[u_1, v_1, p_1](\theta + \Psi = 0, y, \tilde{t}) = [u_1, v_1, p_1](\theta + \Psi = 2\pi, y, \tilde{t}). \tag{2.20}$$

The shift-and-reflect symmetry becomes

$$(u_1, v_1)(\theta + \Psi, y, \tilde{t}) = (u_1, -v_1)(\theta + \Psi + \pi, -y, \tilde{t}).$$

We have

$$\begin{aligned} \boldsymbol{r}^T L\boldsymbol{z} - \boldsymbol{z}^T L^* \boldsymbol{r} = {} & \frac{\partial}{\partial \theta}\left[k(u_0 - U)\{au_1 + bv_1\} + kap_1 + kcu_1\right] \\ & + \frac{\partial}{\partial y}\left[v_0\{au_1 + bv_1\} + bp_1 + cv_1\right], \end{aligned} \tag{2.21}$$

in which

$$L^* = \begin{pmatrix} -\bar{L} + k\dfrac{\partial u_0}{\partial \theta} & k\dfrac{\partial v_0}{\partial \theta} & -k\dfrac{\partial}{\partial \theta} \\ \dfrac{\partial u_0}{\partial y} & -\bar{L} + \dfrac{\partial v_0}{\partial y} & -\dfrac{\partial}{\partial y} \\ -k\dfrac{\partial}{\partial \theta} & -\dfrac{\partial}{\partial y} & 0 \end{pmatrix}, \qquad \boldsymbol{r} = \begin{pmatrix} a \\ b \\ c \end{pmatrix}.$$

Henceforth, the analysis differs from [29]. We define a material volume of fluid Ω bounded in the transverse direction by $y = y_L$ and $y = y_U$ and in the streamwise direction by $\theta + \Psi = 0$ and $\theta + \Psi = 2\pi$, where

$$\psi\left(\theta + \Psi(\tilde{t}), y_L; A(\tilde{t}), B(\tilde{t}), \alpha_0(\tilde{t}), \alpha_1(\tilde{t}), \ldots\right) = -\psi^*, \qquad \psi\left(\theta + \Psi(\tilde{t}), y_U; A(\tilde{t}), B(\tilde{t}), \alpha_0(\tilde{t}), \alpha_1(\tilde{t}), \ldots\right) = \psi^*.$$

The choice of ψ^* is consistent with a constant volume of fluid. The unit outward normal on $\psi = \pm\psi^*$ is given by

$$\hat{\boldsymbol{n}} = \frac{\pm 1}{N}\left(\frac{\partial \psi}{\partial \theta}, \frac{\partial \psi}{\partial y}\right),$$

in which

$$N = \sqrt{\left(\frac{\partial \psi}{\partial \theta}\right)^2 + \left(\frac{\partial \psi}{\partial y}\right)^2}.$$

Equation (2.21) may be integrated to yield

$$\langle \boldsymbol{r}^T L \boldsymbol{z} - \boldsymbol{z}^T L^* \boldsymbol{r} \rangle = I_1 + I_2,$$

where

$$\begin{aligned} \langle\ \boldsymbol{\cdot}\ \rangle &= \frac{1}{\Omega}\int_\Omega \boldsymbol{\cdot}\ \mathrm{d}y\mathrm{d}\theta = \frac{1}{\Omega}\int_{\theta=-\Psi}^{2\pi-\Psi}\int_{y=y_L}^{y_U} \boldsymbol{\cdot}\ \mathrm{d}y\mathrm{d}\theta, \\ I_1 &= \frac{1}{\Omega}\int_{\partial\Omega} \{a u_1 + b v_1\}\,(k(u_0 - U), v_0)\cdot\hat{\boldsymbol{n}}\ \mathrm{d}S, \\ I_2 &= \left\langle \frac{\partial}{\partial \theta}\left[k a p_1 + k c u_1\right] + \frac{\partial}{\partial y}\left[b p_1 + c v_1\right] \right\rangle. \end{aligned}$$

The integral $I_1 = 0$ provided

$$[a, b, c](\theta + \Psi, y, \tilde{t}) = [a, b, c](\theta + \Psi - 2n\pi, y, \tilde{t}). \tag{2.22}$$

It follows from this that if

$$L^* \boldsymbol{r} = \boldsymbol{0}, \tag{2.23}$$

subject to the boundary conditions (2.22), then our linear problem for the first correction can only have a solution if

$$\left\langle a\left(\frac{\partial u_0}{\partial \tilde{t}} - \Delta_0 u_0 - 2\right) + b\left(\frac{\partial v_0}{\partial \tilde{t}} - \Delta_0 v_0\right)\right\rangle = -I_2 \tag{2.24}$$

for any $\boldsymbol{r}$. Four linearly independent solutions of the adjoint problem (2.23) and (2.22) have been determined in [29]:

$$\boldsymbol{r}_1 = (0, 0, 1)^T, \qquad \boldsymbol{r}_2 = (1, 0, u_0)^T, \qquad \boldsymbol{r}_3 = (0, 1, v_0)^T, \qquad \boldsymbol{r}_4 = (u_0, v_0, p_0 + E_0)^T.$$

We now consider a fifth uncountably infinite family of solutions which have only recently been determined:

$$\boldsymbol{r}_5 = \left(\frac{\partial}{\partial y}(\omega_0^{m-1}), -k\frac{\partial}{\partial \theta}(\omega_0^{m-1}), -\frac{(m-1)}{m}\omega_0^m\right)^T,$$

for $m > 1$. The function ω_0^m is continuous on $[-\omega_{max}, \omega_{max}]$, where ω_{max} bounds the values of vorticity on the stable manifold. The Weierstrass approximation theorem ensures that a polynomial,

$$p(\omega_0) = a_0 + a_1\omega_0 + \ldots + a_q\omega_0^q,$$

exists which uniformly approximates ω_0^m on $[-\omega_{max}, \omega_{max}]$, that is

$$p(\omega_0) - \hat{\epsilon} < \omega_0^m < p(\omega_0) + \hat{\epsilon},$$

for any $\hat{\epsilon} > 0$. We note that $a_0 = 0$ in our case and consider the vector space of polynomials $p(\omega_0)$ over the field of real numbers. If we construct a basis for this space of polynomials $\{\omega_0^n \mid n \in \mathbb{N}\}$, then all functions in $\{\omega_0^m \mid m \in \mathbb{R},\ m > 1\}$ are uniformly approximated by our basis. Hence, it is sufficient to construct modulation equations for the basis, taking the powers to be natural numbers. A countably infinite family of linearly independent solutions of the adjoint problem (2.23) and (2.22) have been deduced; that is, $\boldsymbol{r}_5$ for m in the natural numbers. Moreover, the shift-and-reflect symmetry condition implies that

$$\omega_0\left(\theta + \Psi(\tilde{t}), y; A(\tilde{t}), B(\tilde{t}), \alpha_0(\tilde{t}), \alpha_1(\tilde{t}), \ldots\right) = -\omega_0\left(\theta + \Psi(\tilde{t}) + \pi, -y; A(\tilde{t}), B(\tilde{t}), \alpha_0(\tilde{t}), \alpha_1(\tilde{t}), \ldots\right).$$

Therefore, the modulation equations for odd powers of vorticity are degenerate. In the analysis which follows, we choose the powers to be even natural numbers in order to form a basis for these polynomials ($m = 2j$).

The second, fourth and fifth solutions correspond to physical modulation equations in this two-dimensional plane Poiseuille flow.

2.4.1. Streamwise momentum modulation equation. If we substitute the second vector $\boldsymbol{r}_2$ into (2.24), then we obtain our first secularity condition

$$\left\langle \frac{\partial u_0}{\partial \tilde{t}} + \frac{\partial}{\partial \theta}[k u_1 u_0] + \frac{\partial}{\partial y}[v_1 u_0] \right\rangle + \left\langle k \frac{\partial p_1}{\partial \theta} \right\rangle = \langle \Delta_0 u_0 \rangle + 2. \tag{2.25}$$

As in [30], we simplify the left-hand side of this secularity condition (2.25) by applying the transport theorem as follows:

$$\frac{\mathrm{d}}{\mathrm{d}t} \int_\Omega u_0 \ \mathrm{d}y\mathrm{d}\theta = \int_\Omega \frac{\partial u_0}{\partial t} + \boldsymbol{\nabla \cdot}(\boldsymbol{q} u_0) \ \mathrm{d}y\mathrm{d}\theta.$$

We expand this equation to obtain the rate of change of streamwise momentum

$$\frac{\mathrm{d}}{\mathrm{d}\tilde{t}} \int_\Omega u_0 \ \mathrm{d}y\mathrm{d}\theta = \int_\Omega \frac{\partial u_0}{\partial \tilde{t}} + \frac{\partial}{\partial \theta}[k u_1 u_0] + \frac{\partial}{\partial y}[v_1 u_0] \ \mathrm{d}y\mathrm{d}\theta. \tag{2.26}$$

Substituting (2.26) into (2.25) yields

$$\frac{\mathrm{d}}{\mathrm{d}\tilde{t}}\langle u_0 \rangle + \left\langle k \frac{\partial p_1}{\partial \theta} \right\rangle = -\left\langle \frac{\partial \omega_0}{\partial y} \right\rangle + 2. \tag{2.27}$$

We note that the second term on the left-hand side requires knowledge of the next order. Equation (2.27) may be derived more directly from (2.4).

2.4.2. Kinetic energy modulation equation. If we substitute the fourth vector $\boldsymbol{r}_4$ into (2.24), then we obtain our second secularity condition

$$\left\langle \frac{\partial E_0}{\partial \tilde{t}} + \frac{\partial}{\partial \theta}[k u_0 p_1 + k(p_0 + E_0) u_1] + \frac{\partial}{\partial y}[v_0 p_1 + (p_0 + E_0) v_1] \right\rangle = \langle u_0(\Delta_0 u_0 + 2) + v_0 \Delta_0 v_0 \rangle. \tag{2.28}$$

The expression

$$\left\langle \frac{\partial}{\partial \theta}[k(u_0 - U) p_1 + k p_0 u_1] + \frac{\partial}{\partial y}[v_0 p_1 + p_0 v_1] \right\rangle = 0 \tag{2.29}$$

represents the rate at which the surrounding fluid is doing work on the material volume via the surface pressure, this being zero. Using (2.26) with u_0 replaced by E_0 and (2.29), equation (2.28) may be rewritten as

$$\frac{\mathrm{d}}{\mathrm{d}\tilde{t}}\langle E_0 \rangle + U \left\langle k \frac{\partial p_1}{\partial \theta} \right\rangle = \left\langle k \frac{\partial}{\partial \theta}(v_0 \omega_0) - \frac{\partial}{\partial y}(u_0 \omega_0) - \omega_0^2 \right\rangle + 2\langle u_0 \rangle. \tag{2.30}$$

We note that, as in the case of (2.27), the second term on the left-hand side requires knowledge of the next order. Equation (2.30) may also be derived from (2.5).

2.4.3. Vorticity to the power m modulation equations. If we substitute the fifth vector $\boldsymbol{r}_5$ into (2.24), then we obtain our third secularity condition

$$\left\langle \frac{\partial}{\partial y}(\omega_0^{m-1})\left(\frac{\partial u_0}{\partial \tilde{t}} - \Delta_0 u_0 - 2\right) - k\frac{\partial}{\partial \theta}(\omega_0^{m-1})\left(\frac{\partial v_0}{\partial \tilde{t}} - \Delta_0 v_0\right)\right\rangle$$
$$= -\left\langle \frac{\partial}{\partial \theta}\left[k\frac{\partial}{\partial y}(\omega_0^{m-1})p_1 - ku_1\frac{(m-1)}{m}\omega_0^m\right] + \frac{\partial}{\partial y}\left[-k\frac{\partial}{\partial \theta}(\omega_0^{m-1})p_1 - v_1\frac{(m-1)}{m}\omega_0^m\right]\right\rangle.$$

The modulation equation may be derived from algebraic manipulation of this secularity condition or more directly from (2.6). We have

$$\frac{\mathrm{d}}{\mathrm{d}\tilde{t}}\left\langle \omega_0^m \right\rangle = \left\langle m\omega_0^{m-1}\Delta_0\omega_0\right\rangle, \tag{2.31}$$

where $m = 2j$. The right-hand side of equation (2.31) may be rewritten as a double integral of Laplace type

$$\left\langle \omega_0^{m-1}\Delta_0\omega_0\right\rangle = \left\langle \left(\omega_0^{-1}\Delta_0\omega_0\right) e^{j\ln(\omega_0^2)}\right\rangle.$$

A similar comment applies to the integral on the left-hand side of equation (2.31). The maxima of $\ln(\omega_0^2)$ occur along the lower boundary $y = y_L$ and the upper boundary $y = y_U$. It is only the immediate neighbourhood of these two boundaries which contribute to the full asymptotic expansion of these integrals for large values of j. The numerical evaluation of these integrals will require specialized techniques.

2.4.4. Closure. The two ordinary differential equations (2.27) and (2.30) require knowledge of the pressure gradient at next order. This pressure-gradient term may be eliminated to leave a single modulation equation which only involves expressions at leading order. We have

$$\frac{\mathrm{d}}{\mathrm{d}\tilde{t}}\left\langle \hat{E}_0\right\rangle + \frac{\mathrm{d}U}{\mathrm{d}\tilde{t}}\langle \hat{u}_0\rangle = \left\langle k\frac{\partial}{\partial\theta}(v_0\omega_0) - \frac{\partial}{\partial y}\left(\hat{u}_0\omega_0\right) - \omega_0^2\right\rangle + 2\langle \hat{u}_0\rangle, \tag{2.32}$$

where $\hat{u}_0 = u_0 - U$ and $\hat{E}_0 = [\hat{u}_0^2 + v_0^2]/2$. The phase velocity only occurs on the left-hand side of (2.32).

There are a finite number of degrees of freedom and an infinite number of modulation equations. We have an overdetermined system. Equation (2.32) determines the rate of change of U and uncouples. We only require the first $\mathcal{N}+3$ amplitude modulation equations to form a closed system of ordinary differential equations for the evolution of $\{A, B, \alpha_0, \alpha_1, \ldots, \alpha_{\mathcal{N}}\}$. We are disregarding the remaining amplitude modulation equations as they correspond to the higher-order harmonics.

The one issue which remains unresolved in the asymptotic analysis is the sufficiency of the modulation equations. It has not been possible to obtain a general solution to the adjoint problem. A second approach, which would demonstrate sufficiency, is to match the number of modulation equations to the number of slowly varying unknowns. However, this match is also problematic due to the numerical challenges of solving our system at such large Reynolds numbers. In the absence of rigid boundaries, stable travelling waves occur at much lower Reynolds numbers, for example, in Kolmogorov flow. It has been possible to show that the modulation equations above are sufficient in predicting Kolmogorov flow [32].

3. Discussion.

3.1. Physical interpretation. The modulation equations provide us with insight into the physical mechanisms on the long viscous time scale (denoted by the dashed line in Figure 3). The uncoupling of the modulation equation for the averaged kinetic energy and momentum (2.32) means that the dynamics of the amplitude parameters $\{A, B, \alpha_0, \alpha_1, \ldots, \alpha_{\mathcal{N}}\}$ are entirely determined by the averaged powers of vorticity (2.31). We utilize the numerical solution in [33] to illustrate the interchange between the amplitude parameters (with $\epsilon = 2.5\times10^{-4}$, $k = 1.25$ and on a 200×200 mesh). Figure 5 shows a trajectory in the stable manifold of quasi-steady travelling waves projected onto two three-dimensional parameter spaces; the trajectory spirals towards its steady state. The phase velocity responds to these changes in amplitude parameters in such a way that the averaged kinetic energy and momentum are conserved, this being shown in Figure 6. In essence, the vorticity field dictates the dynamics of the amplitude envelope on the long time scale and the phase velocity takes a servile role.

The travelling wave which is eventually attained corresponds to a periodic attractor of the Navier–Stokes equations (denoted by the large dot in Figure 3). The final values of the amplitude parameters must satisfy the equations

$$\left\langle k\frac{\partial}{\partial\theta}(v_0\omega_0) - \frac{\partial}{\partial y}\left(\hat{u}_0\omega_0\right) - \omega_0^2\right\rangle + 2\langle \hat{u}_0\rangle = 0, \qquad \left\langle \omega_0^{m-1}\Delta_0\omega_0\right\rangle = 0. \tag{3.1}$$

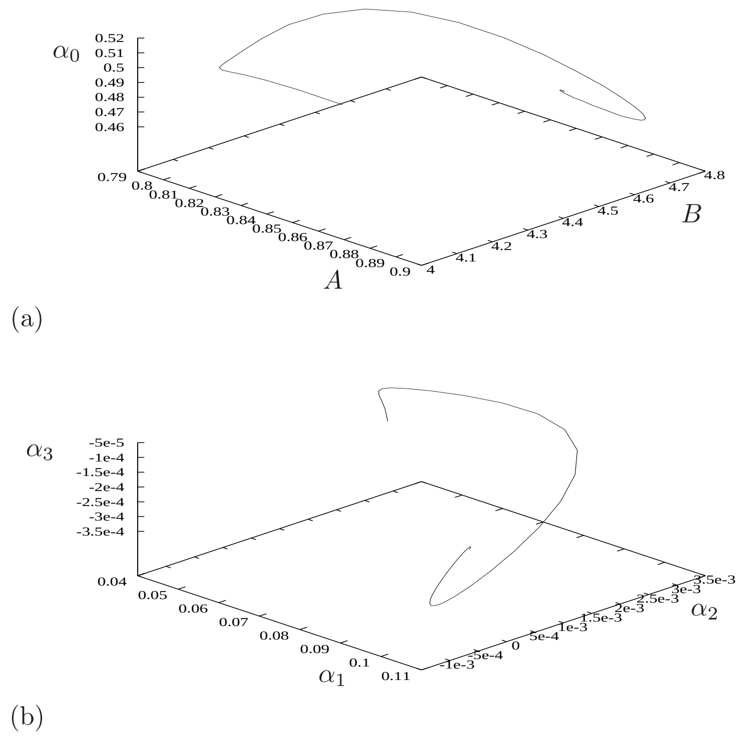

Fig. 5. *A trajectory in the stable manifold of quasi-steady travelling waves visualized using two three-dimensional projections in (a) (A, B, α_0) and (b) (α_1, α_2, α_3) with $\epsilon = 2.5 \times 10^{-4}$ ($R = 4000$) and $k = 1.25$. The interchange between these amplitude parameters is governed by the modulation equations for averaged vorticity (2.31) in which the powers m are taken to be even natural numbers.*

The second equation in (3.1) with $m = 2j$ specifies the manifold in phase space on which the periodic attractor may be found. Once a periodic attractor has been determined, then the first equation in (3.1) should be verified. The phase velocity does not appear in the system (3.1): it is determined by the transient problem.

3.2. Longer domains. In the case of longer domains, the travelling waves studied in this article may not be stable. The dominant stable structures are localized wave packets (see, for example, [7, 24]). Our current asymptotic analysis does not apply to these wave packets. It would be necessary to introduce an asymptotically longer space scale in order to describe them; however, this extension is not straightforward. Fortunately, in some regions of parameter space corresponding to longer domains, the local attractors are uniform wave trains to leading order. The preceding analysis will still be appropriate for these local attractors provided that the maximum-entropy and symmetry conditions still hold.

A long-domain simulation was undertaken for $\epsilon = 2.5 \times 10^{-4}$ ($R = 4000$) and $k = 0.39$. Figure 7 shows a snapshot of the vorticity contours and streamlines for a quasi-steady wave train in a coordinate system moving with the phase velocity. In Figure 7, the first wavelength is a maximum-entropy configuration with $A = 1.084$, $B = 2.460$ and $U = 0.2515$; the second with $A = 1.084$, $B = 2.461$ and $U = 0.2516$; and the third with $A = 1.084$, $B = 2.461$ and $U = 0.2515$. The wave train is uniform at leading order. Figure 7 also serves to demonstrate the validity of the shift-and-reflect symmetry and parity conditions required in the analysis. Therefore the asymptotic structure applies in each of the three cells on this longer domain.

3.3. Three-dimensional problem. We now interpret the implications of our results for the three-dimensional problem with periodic boundary conditions in the third dimension. The three steps in the instability process of [23] are given by

(i) primary (linear) instability of the basic shear flow;
(ii) nonlinear saturation of the primary instability and formation of a secondary flow;
(iii) secondary instability.

The slow evolution of two-dimensional quasi-steady states studied here correspond to the formation of a secondary flow in step (ii). We denote the two-dimensional travelling wave (or secondary flow) by TW and the stable manifold of two-dimensional quasi-steady states by $W^S(TW)$. The finite set of independent slowly varying parameters define

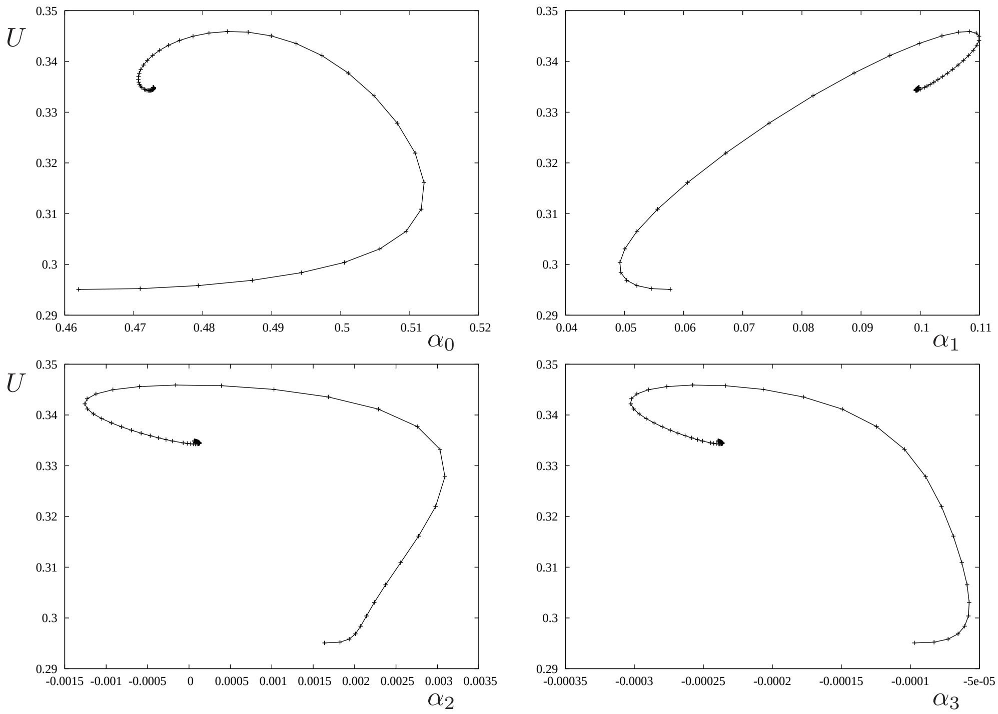

FIG. 6. *A trajectory in the stable manifold of quasi-steady travelling waves visualized using four two-dimensional projections in the* (α_0, U), (α_1, U), (α_2, U) *and* (α_3, U) *planes with* $\epsilon = 2.5 \times 10^{-4}$ ($R = 4000$) *and* $k = 1.25$. *The response of the phase velocity* U *to the changes in the amplitude parameters is governed by the modulation equation for averaged kinetic energy and momentum (2.32).*

the location on this stable manifold with the first seven parameters spiralling towards the steady state value TW. Step (iii) corresponds to the rapid departure of the flow along the unstable manifold $W^U(TW)$. This rapid departure may well occur via three-dimensional coherent states which scale according to vortex-wave interaction theory [10]. We deduce that the flow dynamics of steps (ii) and (iii) correspond to a generalized saddle focus in phase space as shown in Figure 8.

3.4. Two-phased waves. The asymptotic analysis in this article considers a modulated travelling wave with a single phase. As the Reynolds number is increased, this flow undergoes a supercritical Hopf bifurcation and acquires a new frequency or phase (see Figure 1(a)). Figure 9 shows a snapshot of the vorticity contours and streamlines for a quasi-steady travelling wave in a coordinate system moving with the primary phase velocity at a higher Reynolds number than Figure 2. We first note that the shift-and-reflect symmetry was broken at the Hopf bifurcation. Secondly, the viscous boundary layers are no longer passive. Vortex sheets are ejected from the walls into the body of the flow, this physical mechanism having been described in detail elsewhere (using constant mass flux instead of constant pressure gradient [13]). The boundary layers now exert a controlling influence on the flow as a whole and the modulation equations are inapplicable.

We adopt the space-integrated modulus of the vorticity on the lower wall,

$$\bar{\omega} = \int_{x=0}^{2\pi/k} |\omega(x, -1, t)| \mathrm{d}x,$$

to assess the time dependence. It is constant below the bifurcation, but oscillates periodically above. Figure 10(a) shows this variable over a few oscillations which indicates that Figure 9 corresponds to a two-phased travelling wave (or a quasi-periodic attractor). The bifurcation diagram in Figure 1(c) has been modified to Figure 1(d) at a Reynolds number above the first Hopf bifurcation and below the second. We note that the modulation equations will be valid for the intervals of wavenumber corresponding to stable single-phased travelling waves in Figure 1(d), for example, at $R = 15000$ and $k = 1.5$ as reported in [15].

Figure 10(b) shows the vorticity versus the stream function in a coordinate system moving with the primary phase velocity. This is numerical confirmation of the result in [33] that no functional exists between the vorticity and stream function in this reference frame. Attempts to determine maximum-entropy configurations in other reference frames have been unsuccessful. The two-phased wave has lost all the properties which made the single-phased wave tractable.

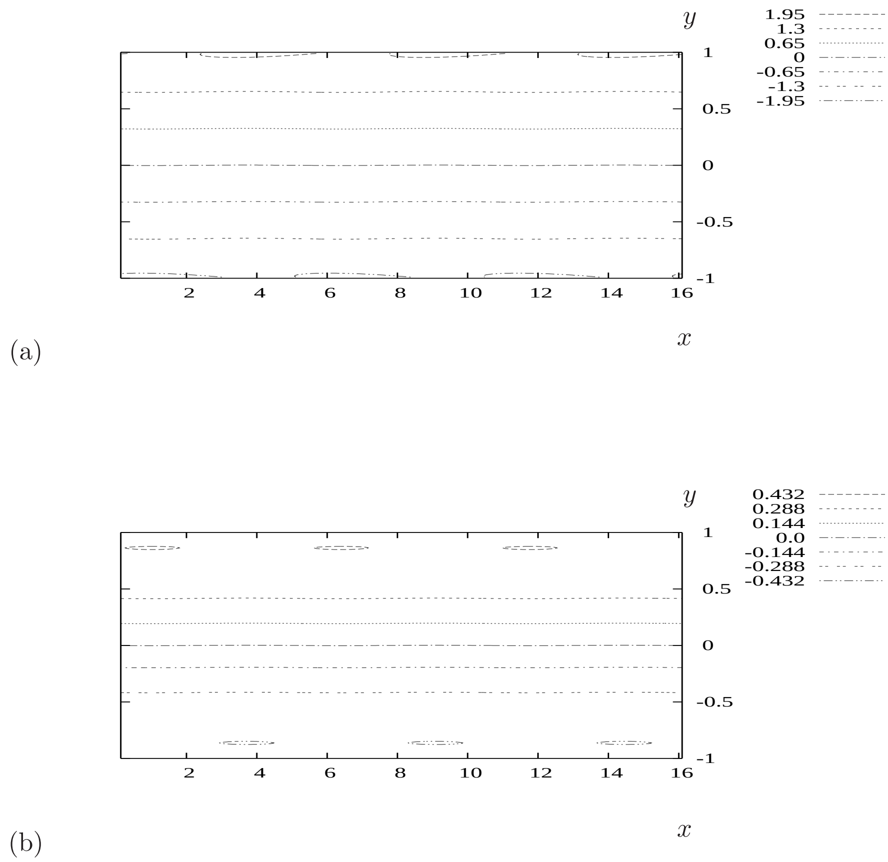

FIG. 7. *Snapshot of vorticity contours (a) and streamlines (b) for a quasi-steady uniform wave train with* $\epsilon = 2.5\times10^{-4}$ *(*$R = 4000$*) and* $k = 0.39$ *plotted in a coordinate system moving with the phase velocity. This solution contains three basic wavelengths.*

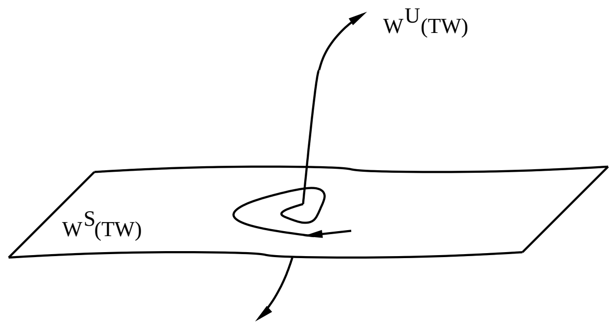

FIG. 8. *A schematic of the generalized saddle focus in phase space describing secondary instability in three-dimensional plane Poiseuille flow, where* TW *is the two-dimensional travelling wave,* $W^S(TW)$ *the stable manifold of two-dimensional quasi-steady states (step (ii) of [23]) and* $W^U(TW)$ *the unstable manifold of three-dimensional states (step (iii) of [23]).*

4. High-temperature limit. In this limit, we assume a linear vorticity-stream function relationship, namely $\omega_0 = AB\psi$. There are two reasons to consider this limit: (i) a general solution of the leading-order outer problem may be obtained; and (ii) the amplitude modulation equations may be integrated analytically.

4.1. The leading-order outer solution. In this limit, equation (2.11) becomes

$$k^2\frac{\partial^2\psi}{\partial\theta^2} + \frac{\partial^2\psi}{\partial y^2} + AB\psi = 0.$$

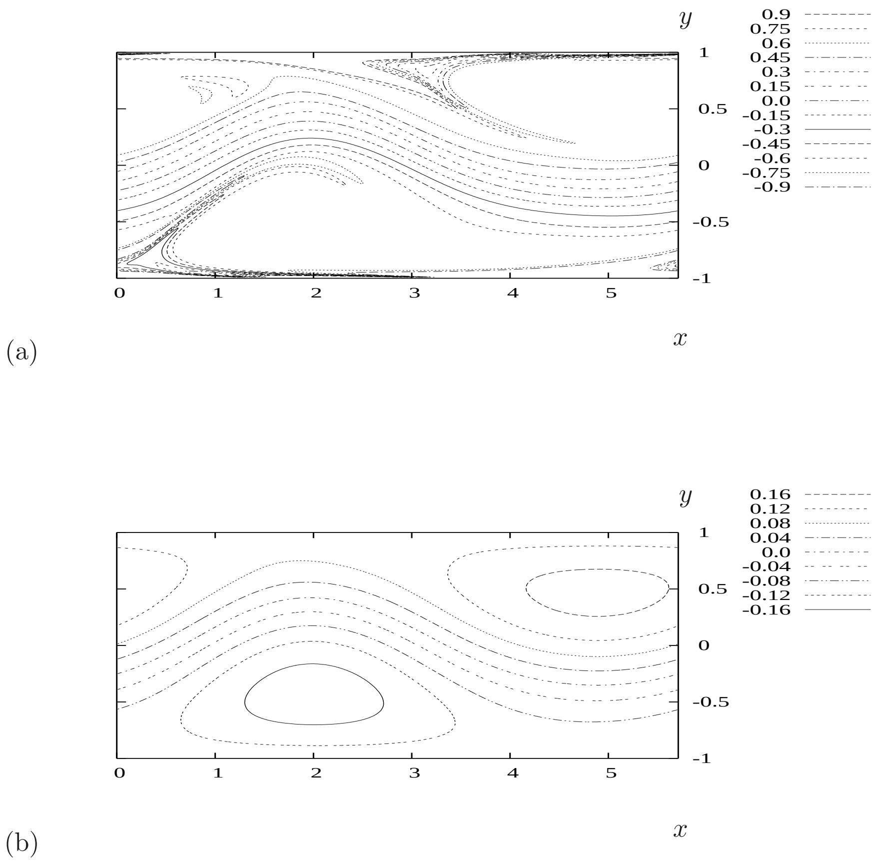

FIG. 9. *Snapshot of vorticity contours (a) and streamlines (b) for a quasi-steady two-phased travelling wave with* $\epsilon = 6.7 \times 10^{-5}$ *(*$R = 15000$*) and* $k = 1.1$ *plotted in a coordinate system moving with the primary phase velocity.*

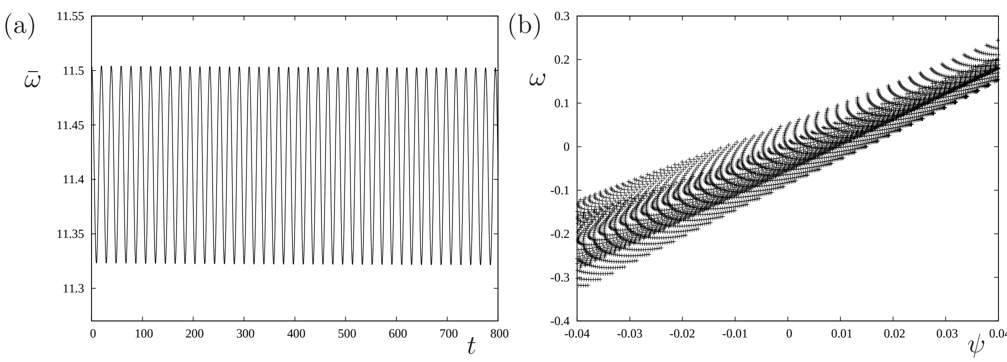

FIG. 10. *Two plots resulting from the simulation described in Figure 9: (a) the space-integrated modulus of the vorticity on the lower wall as a function of time; and (b) scatter plot of the vorticity versus the stream function in a coordinate system moving with the primary phase velocity.*

A general solution of this Helmholtz equation consistent with (2.12)-(2.14) and $k^2 \le AB \le 4k^2$ is

$$\begin{aligned}\psi = &\frac{\alpha_0(\tilde{t})}{\mu_0}\sin(\mu_0 y) + \alpha_1(\tilde{t})\cos(\theta+\Psi)\cos(\mu_1 y)\\ &+ \sum_{l=1}^{l_{even}} \frac{\alpha_{2l}(\tilde{t})}{\mu_{2l}}\cos(2l(\theta+\Psi))\sinh(\mu_{2l}y) + \sum_{l=1}^{l_{odd}} \alpha_{2l+1}(\tilde{t})\cos((2l+1)(\theta+\Psi))\cosh(\mu_{2l+1}y),\end{aligned}$$

where $2l_{even}$ is the largest even number less than or equal to $\mathcal{N}$, $2l_{odd}+1$ is the largest odd number less than or equal to $\mathcal{N}$, $\mu_0 = \sqrt{AB}$, $\mu_1 = \sqrt{AB-k^2}$ and $\mu_l = \sqrt{l^2k^2 - AB}$ for $l \geq 2$. The α_l are the functions defined in (2.17)-(2.18). This general solution serves to illustrate the slowly varying parameters. Unfortunately, we may not exploit this solution to find an approximation to the modulation equations, this being described below.

4.2. Amplitude modulation equations. Using the equation $\omega_0 = AB\psi$, it may be readily shown that $\Delta_0\omega_0 = -AB\omega_0$. The modulation equations (2.31) may then be simplified to become

$$\frac{\mathrm{d}}{\mathrm{d}\tilde{t}} \left\langle \omega_0^{2j} \right\rangle = -mAB \left\langle \omega_0^{2j} \right\rangle,$$

which is integrated to yield

$$\left\langle \omega_0^{2j} \right\rangle (\tilde{t}) = \left\langle \omega_0^{2j} \right\rangle (0)\ \exp(-mAB\tilde{t}).$$

The zero vorticity state is the only fixed point of this system. The powers of vorticity will decay (or grow) exponentially, this zero vorticity state being a global attractor (repeller). We have an unphysical result for these modulated travelling waves. The importance of the nonlinearity in the vorticity-stream function relationship has been highlighted: the stable non-zero vorticity state, which we sought to approximate, no longer exists in this limit.

5. Conclusions. The asymptotic structure of a modulated travelling wave in two-dimensional flow has been investigated. We draw two main conclusions in relation to the balance between the number of slowly varying unknowns and the number of modulation equations. First, a finite number of independent slowly varying unknowns are identified. Slowly varying parameters arise from three sources: (i) the first source corresponds to the phase velocity; (ii) the Joyce–Montgomery equation requires a further two slowly varying unknowns; and (iii) the integral of the sinh-Poisson equation subject to periodicity, parity, symmetry and viscosity conditions is the third source which requires a finite number of slowly varying parameters, one for each of the orthogonal Fourier modes. These slowly varying unknowns are independent and they are all required to fully parametrize solutions in this subset of the phase space neighbouring the upper-energy branch. Our parameterization of the weakly stable modes describes an attracting set of maximum-entropy configurations. The complementary modes, which have been neglected in this parameterization, are strongly damped.

Secondly, a countably infinite number of modulation equations have been determined for two-dimensional plane Poiseuille flow: one modulation equation, which incorporates averaged kinetic energy and momentum, uncouples to determine the phase velocity; and the remaining averaged vorticity modulation conditions form a system of equations for the amplitude parameters. Only a finite number of these vorticity modulation equations are required to determine the finite number of unknowns. The physical mechanism described above represents a much richer dynamics than the classical modulation of travelling waves. The Landau equation for the amplitude envelope is based on the kinetic energy of the fundamental disturbance: the linear stability is counteracted by the weakly nonlinear interactions [34]. Vorticity has no role in the weakly nonlinear theory; nevertheless, in the amplitude envelope of the strongly nonlinear theory, the vorticity dominates the proceedings. The kinetic energy and momentum have a secondary role: they determine the phase velocity, but only in response to the changes in amplitude.

The system of modulation equations describes analytically, for the first time, a periodic attractor of the Navier–Stokes equations and its stable manifold on the upper-energy branch. A similarity between this laminar flow and two-dimensional turbulent flow will now be highlighted. The equation for the enstrophy corresponds to the physics of the cascade and the equation for the averaged kinetic energy is known to be associated with the inverse cascade (see, for example, [6]). Equivalent equations have been shown to describe a laminar flow on the upper-energy branch directly from the equations of motion.

A word of caution is required regarding the applicability of the analysis. It should be borne in mind that the system of modulation equations applies for order one wavenumber ($k = \mathcal{O}(1)$). In the case of longer domains ($k \ll 1$), the dominant stable structures are localized wave packets. In order to describe these attractors, our modulation equations would need to be extended to include derivatives with respect to an asymptotically long space scale.

The analysis of two-dimensional plane Poiseuille flow has required two new techniques to be introduced into the method of Kuzmak-Luke: (i) An uncountably infinite family of null space vectors have been discovered for the adjoint problem, the Weierstrass approximation theorem being applied to restrict the resulting family of null space vectors to a countably infinite linearly independent subset. (ii) The modulation equations for streamwise momentum and kinetic energy include the pressure gradient at next order. They do not represent independent modulation equations for the leading-order problem despite their origin in independent null space vectors: the two must be combined to eliminate the correction term.

The wider relevance of our analysis will now be discussed. Kolmogorov's 1958 seminar was intended to motivate research on the transition to turbulence. Furthermore he sought to obtain analytical expressions for the laminar attractors of the Navier–Stokes equations which form the backbone of this transition, for example, travelling waves, multi-phased travelling waves and quasi-periodic standing waves. His fifth problem anticipated that high-Reynolds-number asymptotic expansions could approximate these laminar attractors. In this article, we have developed asymptotic techniques which will be able to achieve Kolmogorov's aspirations on the transition to turbulence for flows in the simplest domains and with the simplest forcing. This matter is the subject of active investigation.

We conclude by shedding some light on the most important physical mechanism. The diffusion of vorticity across streamlines has been previously identified as the governing physical mechanism [2]. The modulation equations for the averaged powers of vorticity (2.31) may be rewritten as

$$\frac{\mathrm{d}}{\mathrm{d}\tilde{t}}\left\langle \omega_0^{2j}\right\rangle = -2jB\left\langle \omega_0^{2j}(A^2+\omega_0^2)^{1/2}\right\rangle + 4jB^2\left\langle \omega_0^{2j}\hat{E}_0\right\rangle . \tag{5.1}$$

The system of equations (2.32) and (5.1) may be viewed as the strongly nonlinear generalization of the Landau equation. The first term on the right-hand side of (5.1) represents the viscous dissipation of vorticity. The second term on the right-hand side of (5.1) is the most interesting: it represents the production of vorticity. It is this production term which permits the existence of non-trivial travelling waves (periodic attractors). The interaction of kinetic energy in a reference frame moving with the phase velocity and vorticity is the most crucial physical mechanism. Numerical simulations could not have deduced this physical mechanism; they are only capable of anticipating the existence of modulation equations [13].

Acknowledgement. This project has benefited from the constructive comments of an anonymous referee.

REFERENCES

[1] V. I. Arnol'd, *Kolmogorov's hydrodynamic attractors*, Proc. R. Soc. Lond. A, 434 (1991), pp. 19–22.
[2] B. J. Bayly, S. A. Orszag, and T. Herbert, *Instability mechanisms in shear-flow transition*, Ann. Rev. Fluid Mech., 20 (1988), pp. 359–391.
[3] R. J. Bodonyi, F. T. Smith, and J. Gajjar, *Amplitude-dependent stability of boundary-layer flow with a strongly non-linear critical layer*, IMA J. Appl. Math, 30 (1983), pp. 1–19.
[4] S. J. Chapman, *Subcritical transition in channel flows*, J. Fluid Mech., 451 (2002), pp. 35–97.
[5] K. Deguchi and A. G. Walton, *A swirling spiral wave solution in pipe flow*, J. Fluid Mech., 737 (2013), p. R2.
[6] C. R. Doering and J. D. Gibbon, *Applied Analysis of the Navier-Stokes Equations*, Cambridge University Press, Cambridge, 1995.
[7] A. Drissi, M. Net, and I. Mercader, *Subharmonic instabilities of Tollmien-Schlichting waves in two-dimensional Poiseuille flow*, Phys. Rev. E, 60 (1999), pp. 1781–1791.
[8] J. W. Elliott, F. T. Smith, and S. J. Cowley, *Breakdown of boundary layers: (i) on moving surfaces; (ii) in semi-similar unsteady flow; (iii) in fully unsteady flow*, Geophys. Astrophys. Fluid Dynamics, 25 (1983), pp. 77–138.
[9] J. Gajjar and F. T. Smith, *On the global instability of free disturbances with a time-dependent nonlinear viscous critical layer*, J. Fluid Mech., 157 (1985), pp. 53–77.
[10] P. Hall and F. T. Smith, *On strongly nonlinear vortex/wave interactions in boundary-layer transition*, J. Fluid Mech., 227 (1991), pp. 641–666.
[11] T. Herbert, *Periodic secondary motions in a plane channel*, in Proc. 5th Int. Conf. on Numerical Methods in Fluid Dynamics, A. I. Van de Vooren and P. J. Zandbergen, eds., Springer, 1976, pp. 235–240. Lecture Notes in Physics, vol 59.
[12] N. Itoh, *Secondary instability of laminar flows*, Proc. R. Soc. Lond. A, 375 (1981), pp. 565–578.
[13] J. Jiménez, *Transition to turbulence in two-dimensional Poiseuille flow*, J. Fluid Mech., 218 (1990), pp. 265–297.
[14] J. Jiménez and G. B. Whitham, *An averaged Lagrangian method for dissipative wavetrains*, Proc. R. Soc. Lond. A, 349 (1976), pp. 277–287.
[15] W. B. Jones and D. Montgomery, *Finite amplitude steady states of high Reynolds number 2-D channel flow*, Physica D, 73 (1994), pp. 227–243.
[16] G. R. Joyce and D. Montgomery, *Negative temperature states for a two-dimensional guiding-center plasma*, J. Plasma Phys., 10 (1973), pp. 107–121.
[17] G. E. Kuzmak, *Asymptotic solutions of nonlinear second order differential equations with variable coefficients*, Prikl. Mat. Mekh., 23 (1959), pp. 515–526. (In Russian) J. Appl. Math. Mech., 23 (1959), pp. 730-744.(In English).
[18] M. T. Landahl, *The application of kinematic wave theory to wave trains and packets with small dissipation*, Phys. Fluids, 25 (1982), pp. 1512–1516.
[19] J. C. Luke, *A perturbation method for nonlinear dispersive wave problems*, Proc. Roy. Soc. Lond. A, 292 (1966), pp. 403–412.
[20] D. Montgomery and G. R. Joyce, *Statistical mechanics of negative temperature states*, Phys. Fluids, 17 (1974), pp. 1139–1145.
[21] D. Montgomery, W. H. Matthaeus, W. T. Stribling, D. Martinez, and S. Oughton, *Relaxation in two dimensions and the "sinh-Poisson" equation*, Phys. Fluids A, 4 (1992), pp. 3–6.
[22] S. A. Orszag and A. T. Patera, *Subcritical transition to turbulence in planar shear flows*, in Transition and Turbulence, R. E. Meyer, ed., Academic Press, New York, 1981, pp. 127–146.
[23] ———, *Secondary instability of wall-bounded shear flows*, J. Fluid Mech., 128 (1983), pp. 347–385.
[24] T. Price, M. Brachet, and Y. Pomeau, *Numerical characterization of localized solutions in plane Poisuille flow*, Phys. Fluids A, 5 (1993), pp. 762–764.
[25] F. T. Smith and R. J. Bodonyi, *Amplitude-dependent neutral modes in the Hagen-Poiseuille flow through a circular pipe*, Proc. R. Soc. Lond. A, 384 (1982), pp. 463–489.

[26] ———, *Nonlinear critical layers and their development in streaming-flow stability*, J. Fluid Mech., 118 (1982), pp. 165–185.

[27] F. T. Smith and O. R. Burggraf, *On the development of large-sized short-scaled disturbances in boundary layers*, Proc. R. Soc. Lond. A, 399 (1985), pp. 25–55.

[28] F. T. Smith, D. J. Doorly, and A. P. Rothmayer, *On displacement-thickness, wall-layer and mid-flow scales in turbulent boundary layers, and slugs of vorticity in channel and pipe flows*, Proc. R. Soc. Lond. A, 428 (1990), pp. 255–281.

[29] W. R. Smith, *Modulation equations and Reynolds averaging for finite-amplitude nonlinear waves in an incompressible fluid*, IMA J. Appl. Math., 72 (2007), pp. 923–945.

[30] ———, *Modulation equations for strongly nonlinear oscillations of an incompressible viscous drop*, J. Fluid Mech., 654 (2010), pp. 141–159.

[31] W. R. Smith, J. R. King, B. Tuck, and J. W. Orton, *The single-mode rate equations for semiconductor lasers with thermal effects*, IMA J. Appl. Math., 63 (1999), pp. 1–36.

[32] W. R. Smith and J. G. Wissink, *Kolmogorov's attractors*. In preparation.

[33] ———, *Parameterization of travelling waves in plane Poiseuille flow*, IMA J. Appl. Math., 79 (2014), pp. 22–32.

[34] J. T. Stuart, *On the non-linear mechanics of wave disturbances in stable and unstable parallel flows. Part 1. The basic behaviour in plane Poiseuille flow*, J. Fluid Mech., 9 (1960), pp. 353–370.

[35] J. R. Usher and A. D. D. Craik, *Nonlinear wave interactions in shear flows. Part 1. A variational formulation*, J. Fluid Mech., 66 (1974), pp. 209–221.

[36] G. B. Whitham, *Linear and Nonlinear Waves*, John Wiley & Sons, New York, 1974.